An automated injection system for sub-micron sized channels used in shear-driven-chromatography†'‡

Wim De Malsche,[ab] David Clicq,[b] Hamed Eghbali,[b] Veronika Fekete,[b] Han Gardeniers[a] and Gert Desmet[b]

Received 31st May 2006, Accepted 25th July 2006
First published as an Advance Article on the web 9th August 2006
DOI: 10.1039/b607683a

This paper describes a method to automatically and reproducibly inject sharply delimited sample plugs in the shallow (*i.e.*, sub-micron) channels typically used in shear driven chromatography. The formation of asymmetric plugs, which typically occurs during loading of the sample in wide channels, is circumvented by etching a slit in the middle of the channel that is connected to a micro-well and a vacuum system with syringes for the supply of both the analyte and the mobile phase. The design of the injection slit was supported by a series of CFD simulations to optimize its shape and that of the corresponding injection well. The system was intensively tested experimentally and showed good reproducibility, both for the width and the area of the injected peaks (relative standard deviations are max. 4 and 6%, respectively). The concentration of the injected plug was found to be approximately 80% of the original sample concentration. It was also observed that with the current setup the lower limit of the peak width was about 120 μm. This is a consequence of the fact that the peak width originating from the convection filling step becomes negligible to the contribution of diffusion during the filling and flushing time. Being fully automated and perfectly closed, the presently proposed injection system also paves the way to integrate other functionalities in shear driven chromatography, *i.e.* gradient elution and parallelization.

1 Introduction

Our group has previously reported on the feasibility of shear driven chromatography (SDC).[1–3] The operation principle consists of pressing a substrate with an etched groove against a smooth glass plate, thus creating a channel. Without any pressure drop limitation, a flow in the channel is generated by simply moving one of the 2 substrates, which allows a unique access in the so-called forbidden regions that exist in other LC systems. Due to the fast mass transfer characteristics in these channels, extremely low plate heights can be generated in very short times. Recently, a rotational variant of the approach has also been proposed.[4]

In the SDC experiments in sub-micron channels described thus far, a semi-automated injection procedure was used to insert the sample inside the channels.[5,6] This method consists of manually applying the sample just in front of the channel inlet, after which a plug is injected by moving the wall for a predetermined distance using a high-precision translation stage. Subsequently flushing the pre-channel zone with fresh mobile phase then removes the non-entered sample. This method however presents some drawbacks: since the channel entrance extends to the edge of the chip, the definition of plugs is highly dependent on the dicing quality of the substrate. Furthermore, the method is slow and thus gives rise to peak broadening by diffusion already occurring during injection. The reproducibility is poor because of uncontrolled dilution and the manual handling. The fact that the sample is deposited in the open space before the channel substrate brings along contamination risks and possible changes in sample composition because of partial evaporation of the most volatile sample components. Finally, the method does not allow gradient elution, a functionality that is indispensable to perform complex separations.

In general, the definition of sharply delineated small plugs is a difficult problem in on-chip chromatography. The fact that injections are relatively straightforward to perform in electro-osmotic flow systems, in combination with electrokinetic stacking schemes, is one of the reasons for the success of electrically driven separation systems on a chip.[7] Electrokinetic pinching schemes have been shown to very efficiently prevent tailing and peak deformation.[8–10] Pinching is also possible using pressure-driven or vacuum-driven injections, a method that has been used in combination with capillary electrophoresis on a chip.[11] Another example of the use of pressure to define plugs in a channel is *e.g.* the work of Blom *et al.*[12,13] who designed a method using low resistance supply channels in a high resistance separation channel, in order to minimize the concentration gradient of the introduced plug over the channel width during sample loading. In the case of pressure-driven injections one can decrease injection times and therefore minimize diffusive band broadening by applying high pressures over low flow resistance sample inlets.[14]

[a]*MESA+ Research institute, Enschede, The Netherlands. E-mail: w.malsche@ewi.utwente.nl; Fax: +31 53 489 3595; Tel: +31 53 489 2594*
[b]*Vrije Universiteit Brussel, Department of Chemical Engineering, Brussels, Belgium. E-mail: david.clicq@vub.ac.be; Fax: +32 2 629 3248; Tel: +32 2 629 3318*

† Electronic supplementary information (ESI) available: Fig. S1 (CFD generated flow profiles and peak widths for different well configurations), S2 (top-view of injection sequence) and S3 (peak widths *vs.* different injection translation distances). See DOI: 10.1039/b607683a
‡ The HTML version of this paper has been enhanced with additional colour images.

 This journal is © The Royal Society of Chemistry 2006

In the case of a shear-driven system, the application of high pressure injection flows running directly into the channel is not possible because the pressure would lift the top substrate of the channel. Typically a 0.5 bar normal load pressure is used to keep the separate sandwich channel parts in close contact. This pressure is a trade-off between providing close contact at the interface between stationary and moving substrate and allowing the presence of a lubrication layer to avoid scratching and uncontrolled blocking. In the present study we take advantage of another feature of SDC to develop an automated injection scheme. Since SDC performs best in sub-micron depth channels, the times needed to equilibrate the liquid in the channel with a liquid brought into direct contact with this liquid are extremely short (order of a few milliseconds as can be estimated from Einstein's diffusion law and assuming d = 300 nm and $D_{mol} = 7.96 \times 10^{-10}$ m^2 s^{-1}):

$$t_{diff} = d^2/(2D_{mol}) \quad (1)$$

From this consideration, we have developed a new injection method using an etched inlet slit that enters the channel from the backside of the stationary substrate to bring the sample in direct contact with the liquid occupying the channel space. The slit is connected to a small micro-well that can be filled and emptied in a fast and automated manner. In this paper we will demonstrate that with this setup very narrow sample plugs can be injected within 1 s in a 300 nm deep separation channel, and discuss the factors that determine peak width. The basics of the injection procedure are shown in Fig. 1. Injection consists of the following steps: emptying the micro-well and injection slit, filling with analyte, injection of analyte in channel by moving the substrate over a desired distance at a defined velocity, emptying the micro-well and injection slit, filling the well with mobile phase and finally translating the substrate to start the movement of the injected plug in the channel.

2 Computational fluid dynamics modelling of injection procedure

In order to study the feasibility of the injection procedure depicted in Fig. 1, we have performed 2D fluidic simulations, using the Computational Fluid Dynamics (CFD) software package Fluent® (Fluent N.V., Belgium). The effect of different injection slit shapes and various channel configurations on peak width and concentration of introduced plugs was studied. For the depth of the channel a value of 1 μm was chosen. Only a part of the injection slit (10 μm high) and of the channel (70 μm long) was discretized in space using the grid generator Gambit® (Fluent N.V., Belgium). An injection time of 20 ms was set with a moving wall velocity of 1 mm s^{-1}. Time steps of 1 ms were used to describe the transient behaviour of the plugs. It was checked that refining the grid size and decreasing the time step had no effect on the velocity fields and the mass balances.

A computer simulation of the injection is shown in Fig. 1. Infinite mass transfer is assumed during loading, which corresponds to the use of a fast response syringe and vacuum system in combination with low-resistance supply channels. Unilateral diffusion during loading of the sample gives rise to slightly asymmetric plugs. This approximation of an infinite fast filling speed of the well leads to a linear relation between the injection time (or translated distance) and peak width, except for injection times smaller than 0.01 s where the linear flow profile can no longer be approximated by the average mobile phase velocity.[15]

In order to approximate the likely influence of the injection well shape on the acquired plug widths, simulations were performed for different slit configurations. Remarkably, no differences in peak shape occur when the shape of the slit is altered or when a dead zone or pre-channel is incorporated. This convinced us that one can simply use anisotropic etching of silicon in aqueous KOH solution, giving rise to an injection micro-well with sidewalls sloped at 55°. It turned out, however, that there is an effect on the maximum concentration and width of injected plugs, if the mobile phase cannot be aspirated completely from the bottom of the separation channel. This can occur when a polar solvent has enough affinity for the substrate material, such as silicon which has a native layer of silicon oxide.

3 Experimental

3.1 Chip design and microfabrication procedure

The process for the fabrication of the chip is depicted schematically in Fig. 2. A (100) silicon wafer with a diameter of 10 cm and a thickness of 1 mm was coated with 300 nm silicon-rich silicon nitride, with a standard low pressure chemical vapor deposition (LPCVD) process. At the backside of the wafer rectangular holes were etched in this coating, by reactive ion etching (RIE). Next, the exposed silicon was etched with 25 wt% aqueous KOH to a depth of 850 μm. Spacers used to define the separation channels were

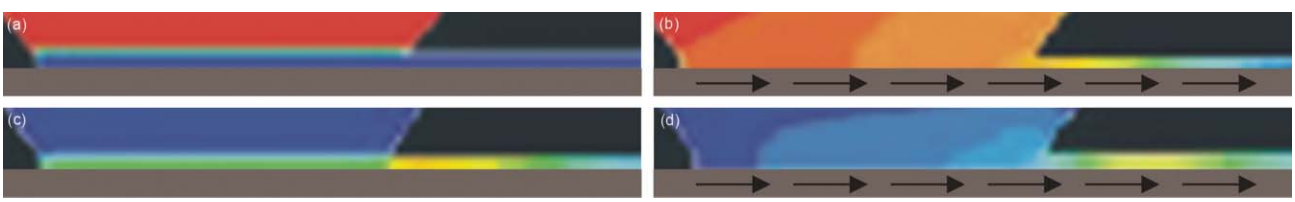

Fig. 1 CFD simulation of the different steps during injection: (a) sample is loaded into the injection slit and micro-well; (b) sample is injected into the channel by displacement of the moving wall at a distance further referred to as injection translation distance (see arrows), *i.e.* the lower part is moved to the right, here the injection translation distance imposes predominantly the defined peak width; (c) sample in the injection slit and micro-well is replaced by mobile phase; (d) the injected plug is transported through the channel by restarting the motion of the movable wall. The color scale ranges from red for the original high, to deep blue for zero concentration of analyte.

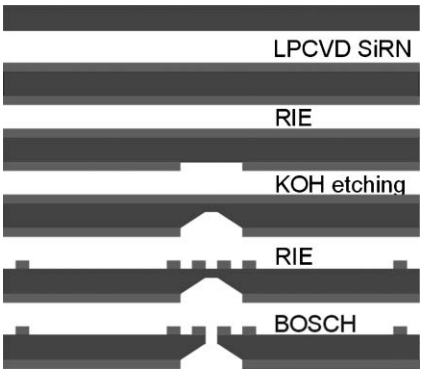

Fig. 2 Process scheme for the fabrication of the chip (not to scale). See text for details.

subsequently fabricated by RIE etching of the silicon nitride layer at the front side of the wafer.

Through-holes were made by Bosch-type deep reactive ion etching, in order to generate the injection slit. Finally, the wafer was diced in chips of 1 cm × 2 cm. Fig. 3b shows a typical example of one of the fabricated injection slits and sample/mobile phase micro-well. In this particular case, a small spacer was left behind the injection slit. Without the spacer, the moving wall would essentially still drag liquid from the front end of the channel and not from the injection well itself. A 2 mm thick polymethylmethoxymetacrylate (PMMA) plate was milled with a high precision milling robot (M7 CNC, Datron, Germany) to define supply channels to the slit. Through holes were produced to connect the system to the sample and mobile phase inlet and to the vacuum system. The patterned silicon substrate and the milled PMMA block were then bonded at room temperature with epoxy glue as an intermediate layer.

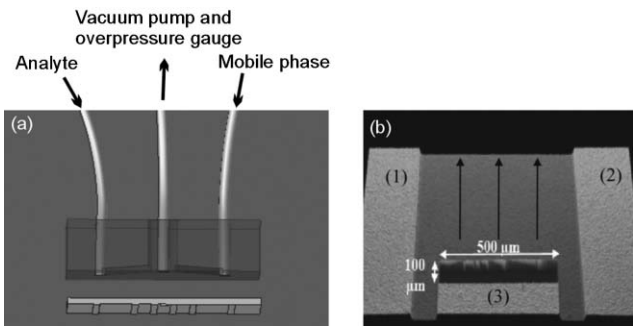

Fig. 3 Outline of the injection system. (a) The PMMA block is glued to the silicon chip and placed on a fused silica substrate (not shown) that serves as a movable wall. The supply channels in the PMMA connect to a cavity above the injection micro-well. The hole for the outlet capillary directly above the well was drilled somewhat larger than the capillary outer diameter to create an overpressure gauge, the other two capillaries are made to fit tightly and leak-free to the holes in the PMMA. (b) Wyko® (optical profilometry) scan of the backside of the etched well, showing the position of the injection slit in the channel, together with the non-etched channel spacer regions (1,2) delimiting the lateral extent of the channel and the non-etched region (3) preventing the mobile phase that is present in front of the channel to enter the channel. The flow direction is indicated by the arrows.

3.2 Injection system and injection procedure

Initially, a closed system was used to ensure that the well was empty before the sample or the mobile phase were introduced and to avoid dilution of the sample. It appeared however that the pressure originating from the syringes was too high to keep the movable substrate and the channel chip in close contact. This problem was solved by providing an opening to release the possible overpressure.

For the movable wall, an ultra-flat fused silica substrate (flatness $\lambda/20$, Photox Optical systems, UK) with a diameter of 5 cm was fixed in a holder which was mounted on a breadboard (M-IG 23-2, Newport B.V., The Netherlands) equipped with a linear displacement stage (M-TS100DC.5, Newport B.V.), a stepping motor (UE611CC, Newport B.V.) and a speed controller (MM4006, Newport B.V.) with a positioning accuracy of 0.5 μm. A channel was defined by pressing the silicon side of the chip on top of it at a pressure of 0.5 bar, firmly fixed in a holder to avoid undesired lateral movements. The PMMA side was connected *via* PEEK capillaries to an automated system of supply syringes and a vacuum pump (Fig. 3).

The movements of the analyte and mobile phase syringes were actuated with stepping motors (respectively Minimotor 2036U024BK1155, 20/1 reductor, Faulhaber S.A., Belgium and M-060, Physik Instruments, Germany). This allowed an easy variation of the generated pressure, the injection distance, the velocity of the moving wall and the timing and duration of the different steps during the injection. The injection procedure consisted in emptying the injection slit and micro-well by use of a vacuum pump, filling both with analyte using a syringe, injecting the analyte in the separation channel by moving the substrate over a specific distance (which was varied, see results) at a velocity of 2 mm s^{-1}, emptying the injection slit and micro-well by vacuum, filling them with mobile phase using a syringe, and finally translating the movable wall at a velocity of 2 mm s^{-1} in order to propagate the injected plug in the channel.

3.3 Chemicals

For the analyte solution 7-diethylamino-4-methylcoumarin (C460, Across Organics, Belgium) was dissolved in HPLC-grade methanol at a final concentration of 10^{-3} M, after which it was filtered. For the mobile phase HPLC-grade methanol was used.

3.4 Detection and plug analysis

To monitor the injections, the objective lens of an inverted microscope (Axiovert 200, Zeiss NV, Belgium) was positioned below the fused silica substrate. For large injected plugs (100, 200 and 300 μm translation distance) the peaks were monitored at 4× magnification, whereas for smaller plugs (100, 50 and 30 μm translation distance) the magnification was 20×. To record the images, an air cooled CCD fluorescence camera (ORCA-ERG C4742-95-12, Hamamatsu Photonics, Belgium) was mounted on the video adapter of the microscope. For excitation of the analyte a Hg-vapour lamp (HBO103/W2, Zeiss, Belgium) was used, along with a UV

 This journal is © The Royal Society of Chemistry 2006

filter cube set (U V-2A DM400 Nikon, Cetec N.V., Belgium). The camera was operated at a frame rate of 15 Hz and the exposure time was 10 ms. Analysis of the video images was performed with simple-PCI ® 5.1 software. A region slightly smaller than the injection slit was vertically squeezed by the software to smoothen the concentration profile, this averages the intensity across the width of the channel. The peaks were fitted as Gaussian shapes using the program Sigmaplot 2000 (SPSS Science, IL, USA).

For the quantitative evaluation of the peak width measurements, the diffusion coefficient of C460 in methanol was determined according to the method of Pappaert *et al.*[16] and found to be $7.96 \times 10^{-10} \pm 0.6 \times 10^{-10}$ m^2 s^{-1}.

4 Results and discussion

Fig. 4 shows a detailed view of the formation process of the injected peak and its evolution through the channel. In curve (1), the movable wall is stopped and the sample present in the slit is replaced by a mobile phase. Considering the curves (2) to (9) it can be seen that the left sides of the curves rapidly decrease in intensity. Curve (10) represents the final shape of the plug at the end of the injection process. The curves (11) to (16) correspond to the different positions of the peak during the actual flow process in the separation channel. As can be noted, the injected peaks become symmetrical within 100 μm of their displacement through the channel.

To characterize the operation of the injection method, different injection translation distances were investigated and the respective resulting peak widths were determined (Table 1). Unfortunately, it was not possible to determine the peak width immediately after the plug is released from the slit because of the strong autofluorescence of the small PMMA piece closing off the injection well. For this reason, the plugs were analyzed at a given distance downstream of the slit. This distance had to be varied because the chips always slightly moved once the load pressure was applied. Depending on which position the width is measured, the difference in peak width can be calculated using

$$H = \Delta\sigma^2/\Delta L = 2D_m/u + (1/15)ud^2/D_m \quad (2)$$

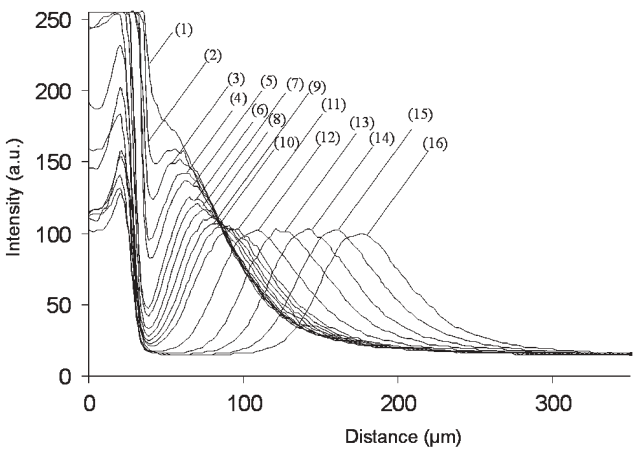

Fig. 4 Formation and evolution of a peak created by an injection with an injection translation distance of 100 μm (time step between consecutive intensity profiles is 23.2 ms). See text for details.

Table 1 Peak widths and relative standard deviations (n = 3) of peak area and peak maximum observed at the respective positions for different injection translation distances

Injection translation distance/μm	Position/ μm	Peak width/μm	RSD peak area	RSD peak max.
300	420	204 ± 1%	3%	1%
200	475	162 ± 1%	3%	3%
100	290	134 ± 1%	1%	4%
100	230	126 ± 1%	3%	7%
50	215	122 ± 4%	2%	1%
30	210	122 ± 3%	6%	6%

with H the plate height, σ the standard deviation of the plug, L the distance the plug has traveled, u the movable wall velocity, d the depth of the channel and D_m the diffusion coefficient. The origin of the factor "1/15" is discussed in ref. 1. Assuming a channel depth of 300 nm, eqn (2) predicts a plate height value of 1.6 μm. This value is then used further on in eqn (8) to compensate for the different measurement positions.

It was observed (see ESI† for more information) that for injection translation distances below 100 μm the finally obtained plug width becomes independent of this distance. For example, no difference is observable between an injection translation distance of 30 μm and 50 μm, both result in peak widths of 122 μm (±3 and 4% RSD, respectively). The timing for the pumping and suction events used to obtain the results depicted in Fig. 4 was the fastest possible with the current set-up. Using shorter filling and emptying sequences, the system went into a regime of irreproducible and tailed injections, due to the incomplete emptying of the well and limited time-response of the vacuum system.

To understand the relation between the injection sequence timing and the injection translation distance on the one hand, and the finally obtained injection plug width, the following consideration can be made.

A quantitative description for the diffusion out of a region during the finite filling times of the injection slit and micro-well is found as follows. As long as the reservoir is filled with sample, the peak width can be expressed as:[17]

$$w^2_{cont} = 5382 D_m t_{cont} \quad (3)$$

wherein t_{cont} is the total time during which the sample is in contact with the mobile phase occupying the rest of the channel:

$$t_{cont} = t_{fill} + z/u \quad (4)$$

In eqn (3), the peak width w is expressed as being equal to 4 times σ, the square root of the second moment of the concentration *vs.* position profile.

The contribution due to movement of the movable wall during the injection is determined by the average distance (w_{conv}) over which the mobile phase has moved, which is half the injection translation distance of the movable wall (z):

$$w_{conv} = z/2 \quad (5)$$

The band broadening of the plug while remaining in place inside the channel during the flushing step can be derived from Einstein's diffusion law (eqn (1)) and is given by:[18]

$$w_{\text{flush}} = (32Dt_{\text{flush}})^{1/2} \quad (6)$$

The total peak width w_{inj} immedialy after the completion of the injection step is then found using:

$$w_{\text{inj}}^2 = w_{\text{cont}}^2 + w_{\text{conv}}^2 + w_{\text{flush}}^2 \quad (7)$$

The additional band broadening experienced during the movement of the plug over a distance x in the channel is then given by the product of the plate height H calculated with eqn (2) and the average distance x over which the plug has moved, yielding for the final plug width:

$$\Delta w = 4(w_{\text{inj}}^2/16 + Hx)^{1/2} \quad (8)$$

The above analysis has made it clear that the system variables t_{fill} and t_{flush} impose the minimal width of an injected plug. Roughly estimating these times as being respectively 0.2 s and 0.3 s, this gives rise to numerical values of respectively 29 μm and 87 μm and thus a total value of 92 μm. It is also important to notice that according to eqn (2) smaller peaks give rise to a larger relative broadening. After having traveled 210 μm in the channel (this position is the reference value to compare experimentally determined peak widths), then an increase of 21 μm in width will occur. The total minimal peak width at our observation position is then 113 μm. Deviations of this model are mostly due to the approximation made in eqn (5) and the uncertainty on the duration of the different steps.

In summary, the good agreement between the theoretical verification and the experimental results obtained implies that eqns (2)–(8) provide a good model to predicit the injection peak width.

A crucial factor determining the success of an injection method for an analytical device is its reproducibility. Fig. 5b shows the fluorescence intensity profiles for three consecutive injections using the manual procedure described by Desmet *et al.*[17] As can be noted, the width of the injected plugs is relatively reproducible, but the intensity clearly is not. This is essentially due to slight variations in mobile phase drops remaining on the front of the channel substrate during the sample deposition. Depending on the magnitude of these drops, the deposited sample gets more diluted or less diluted, resulting in significant changes of the finally injected sample concentration. Another factor is the dependence on the dicing quality, which leads to non-rectangular peaks in top-view. This is not the case in the automated system. Fig. 5a shows that the reproducibility of the injected sample plug width and concentration offered by the currently developed automated injection slit system is much better than with the semi-automated approach used in ref. 18. As indicated in Table 1, the RSD on the injection width was on the order of 1%, except for the smallest peaks where diffusion plays a significant role and where the standard deviation was on the order of 4%. The RSD on the amount of injected sample was of the order of 3% for all the injections, except for the 30 μm injection translation distance, where a value of 6% RSD was found.

Fitting the peaks in Fig. 5a with a Gaussian curve showed that the injected peaks are nearly perfectly Gaussian. Although the run-to-run reproducibility of the injected concentration is quite good, the final sample concentration depends on the injected peak width. This is due to the dilution effects occurring during the flushing step of the injection (see curves 2–9 in Fig. 4) caused by contact with the residual mobile phase in the supply channels and the micro-well that remain as a wetting layer. The peak concentration as measured for a 100 μm plug was 80% (as compared to the fluorescence signal of a continuously introduced sample solution) of the sample concentration. For the smaller peaks the decrease was even stronger.

5 Conclusions

Using the presented chip layout and the combined vacuum and shear driven system, reproducible and undisturbed plugs have been injected with good reproducibility (relative standard deviations were max. 4 and 6% for width and area, respectively, and were in some runs even equal to 1%). This is

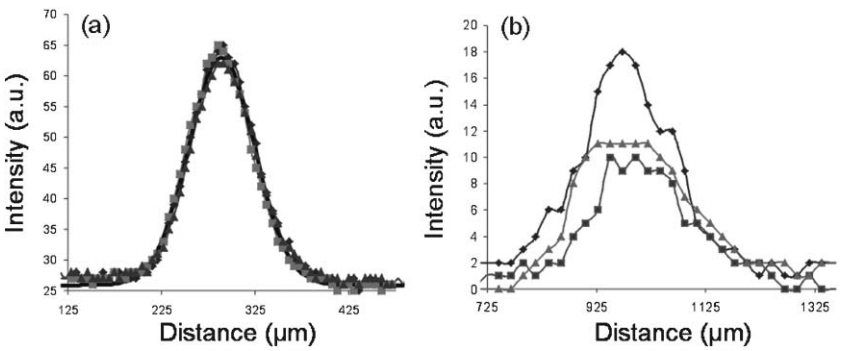

Fig. 5 (a) Repetition of 3 peaks generated by translating the movable substrate for a distance of 100 micron using the automated injection slit method. The thick line represents the average of the gauss fits of these experimental curves. The relative standard deviations of the peak width and peak area are both 1%. (b) Repetition of 3 injected peaks using the semi-automated channel front injection procedure described by Desmet *et al.*[17] For the injection, the movable wall was translated over a distance of 100 μm. The plugs of 6×10^{-4} M FITC in methanol have traveled 975 μm after being injected. The variances of the peak width and peak area are respectively 12 and 27%.

 This journal is © The Royal Society of Chemistry 2006

an important asset for shear driven chromatography, as the analytical use of the system has always been hindered by the inability to perform reproducible injections. The semi-automated injections as performed in the past have always been shown to be substrate dependent, since dicing quality differs considerably between different chips, and because of the human aspects of the injection. Apart from the variable timing of the consecutive injection steps used in different experiments, the unreliable positioning of the externally positioned mobile phase, sample needles, and of the vacuum system tube contributed to peak width and peak height variances. The most important variance came from uncontrolled dilution, as seen in the large difference in peak areas (RSD of 27% for the old system as compared to a maximum of 6% for the currently presented fully automated system). Another significant advantage of the new system (not realized in the present study however) is the ability to change the mobile phase concentration during a separation experiment in a controlled fashion and to perform gradient elution separations of complex mixtures.

Acknowledgements

The authors would like to thank Dr ir. Kris Pappaert for help with the determination of the diffusion coefficient of C460.

References

1 G. Desmet and G. V. Baron, *J. Chromatogr., A*, 1999, **855**, 57–70.
2 G. Desmet and G. V. Baron, *J. Chromatogr., A*, 2000, **867**, 23–43.
3 G. Desmet, N. Vervoort, D. Clicq and G. V. Baron, *J. Chromatogr., A*, 2001, **924**, 111–122.
4 X. Yang, G. Jenkins, J. Franzke and A. Manz, *Lab Chip*, 2005, **5**, 764–771.
5 D. Clicq, S. Vankrunkelsven, W. Ranson, C. De Tandt, G. V. Baron and G. Desmet, *Anal. Chim. Acta*, 2004, **507**, 79–86.
6 D. Clicq, N. Vervoort, R. Vounckx, H. Ottevaere, J. Buijs, C. Gooijer, F. Ariese, G. V. Baron and G. Desmet, *J. Chromatogr., A*, 2002, **979**, 33–42.
7 J. P. Kutter and Y. Fintschenko, *Separation Methods in Microanalytical Systems*, Taylor and Francis, Boca Raton, 2006.
8 S. C. Jacobsen, R. Hergenroder, L. B. Koutney, R. Warmack and J. M. Ramsey, *Anal. Chem.*, 1994, **66**, 1107–1113.
9 S. C. Jacobsen, R. Hergenroder, L. B. Koutney, R. Warmack and J. M. Ramsey, *Anal. Chem.*, 1994, **66**, 1114–1118.
10 C. D. Thomas, S. C. Jacobson and J. M. Ramsey, *Anal. Chem.*, 2004, **76**, 6053–6057.
11 S. C. Jacobson and J. M. Ramsey, *Electrophoresis*, 1995, **16**, 481–486.
12 M. T. Blom, E. Chmela, J. G. E. Gardeniers, R. Tijssen, M. Elwenspoek and A. van den Berg, *Sens. Actuators, B*, 2002, **82**, 111–116.
13 M. T. Blom, E. Chmela, R. E. Oosterbroek, R. Tijssen and A. van den Berg, *Anal. Chem.*, 2003, **75**, 6761–6768.
14 A. P. O'Neill, P. O'Brien, J. Alderman, D. Hoffman, M. McEnery, J. Murrihy and J. D. Glennon, *J. Chromatogr. A*, 2001, **924**, 259–263.
15 W. De Malsche, D. Clicq, H. Eghbali, N. Vervoort, J. G. E. Gardeniers, A. van den Berg and G. Desmet, *Proceedings of μTAS 2005*, Boston, MA, USA, Transducer Research Foundation, San Diego, CA, USA, 2005, pp. 106–108.
16 K. Pappaert, J. Biesemans, D. Clicq, S. Vankrunkelsven and G. Desmet, *Lab Chip*, 2005, **5**, 1104–1110.
17 G. Desmet, N. Vervoort, D. Clicq, A. Huau, P. Gzil and G. V. Baron, *J. Chromatogr. A*, 2002, **948**, 19–34.
18 J. C. Giddings, *Unified Separation Science*, John Wiley & Sons, Inc., New York, 1991.

This journal is © The Royal Society of Chemistry 2006